Electrical Power and Energy Systems 165 (2025) 110467

Contents lists available at ScienceDirect

International Journal of Electrical Power and Energy Systems

journal homepage: www.elsevier.com/locate/ijepes

Addressing intra-area oscillations and frequency stability after DC segmentation of a large AC power system

M. Robin [a,b], J. Renedo [c], J.C. Gonzalez-Torres [a], A. Garcia-Cerrada [b,*], L. Rouco [b], A. Benchaib [a], P. Garcia-Gonzalez [b]

[a] SuperGrid Institute, 23 Rue Cyprian, Villeurbanne, 69100, France
[b] Instituto de Investigación Tecnológica (IIT), ETSI ICAI, Universidad Pontificia Comillas, Alberto Aguilera 23, Madrid, 28015, Spain
[c] ETSI ICAI, Universidad Pontificia Comillas, Alberto Aguilera 23, Madrid, 28015, Spain

ARTICLE INFO

Keywords:
HVAC/HVDC
Voltage source converter
VSC-HVDC
Power system stability
DC segmentation
Power-oscillation damping
POD-Q
Frequency control

ABSTRACT

Several events have shown that electromechanical oscillations are a major concern for large interconnected Alternating Current (AC) power systems. Segmentation of AC power systems with High Voltage Direct Current (HVDC) systems (DC segmentation, for short) turns large AC grids into a set of asynchronous AC clusters linked by HVDC links. It is a promising solution to mitigate electromechanical oscillations and other issues. In particular, an appropriate placement of DC segmentation can stop a selected inter-area electromechanical oscillation mode. However, without supplementary controllers, DC segmentation will not contribute to the damping of the intra-area oscillation modes in the remaining AC clusters and frequency stability of the overall system will deteriorate. This paper studies the use of DC segmentation with HVDC systems based on Voltage Source Converters (VSC-HVDC) with active and reactive power supplementary controllers in the converter stations. The former were tailored for frequency support among the asynchronous AC clusters and the latter for Power-Oscillation Damping (POD-Q) of the intra-area oscillation modes. The proposed supplementary controllers and their design will be presented, and their efficiency will be demonstrated on the Nordic 44 test system with DC segmentation by means of non-linear time-domain simulation and small-signal stability analysis.

1. Introduction

Alternating Current (AC) technology is currently the dominant technology for the transmission and distribution of electrical energy. However, transmission capability with High Voltage Alternating Current (HVAC) is limited by some technical aspects that can be overcome by using the High Voltage Direct Current (HVDC) transmission technology developed in the last decades [1]. Thus, many point-to-point HVDC links are already in operation around the world, and even more are planned or under construction [2,3]. This means that electrical grids are evolving towards hybrid HVAC/HVDC power systems with a growing share of HVDC transmission [4].

In parallel with the development of HVDC links, power systems have also become more and more interconnected creating large AC synchronous electrical grids. This action sums the interconnected systems' inertia values, improves frequency stability and increases the reliability of the resulting power systems. However, with the introduction of new economical objectives, power systems are operated closer to their stability limits and the risk of severe disruptions is increasing rapidly. For example, in the last decade, several events have shown that electromechanical oscillations are now a bigger threat than ever [5]. Electromechanical oscillations are a rotor-angle stability phenomenon under small perturbations in a frequency range between 0.1 and 2 Hz (low-frequency oscillations) [6].

Traditionally, the most cost-effective solution to damp electromechanical oscillations in power systems has been the use of supplementary controllers attached in the different devices of the power system. The most extended solution is the implementation of Power System Stabilizers (PSS) in synchronous machines [7]. Nevertheless, supplementary Power-Oscillation Damping (POD) controllers in renewable power plants [8,9], Energy Storage Systems (ESS) [10], Flexible Alternating Current Transmission Systems (FACTS) devices [11,12], and HVDC systems based on Line Commutated Converters (LCC-HVDC) [13] or based on Voltage Source Converters (VSC-HVDC) [14–19] have also proved to be effective solutions.

* Corresponding author.
E-mail address: aurelio@comillas.edu (A. Garcia-Cerrada).

https://doi.org/10.1016/j.ijepes.2025.110467
Received 4 October 2024; Received in revised form 17 December 2024; Accepted 6 January 2025
Available online 18 January 2025

In stressed power systems, electromechanical oscillations with low damping ratio can arise in certain scenarios, even if dedicated supplementary controllers are attached in the different devices of the power system. In these situations, corrective actions, such as reduction of power exchange between the different areas, may be necessary as occurred on 1 December 2016 in the CE (continental Europe) power system [5]. In extremely severe cases, other corrective actions such as intentional islanding have been proposed. Intentional islanding will disconnect selected lines to split a grid into a set of stable areas – called islands – that are reconnected once the fault and its propagation have been addressed properly [20–23].

Intentional islanding is only an operational action that is not meant to be permanent.

However, recent work has analysed the segmentation of AC power systems with VSC-HVDC links (DC segmentation, for short) to mitigate electromechanical oscillations [24], which is a potential permanent solution to be undertaken in stressed power systems when planning a system upgrade. DC segmentation was first proposed in [25] and consists in segmenting a large AC asynchronous grid into a set of AC asynchronous grids linked by HVDC links. It is regarded as a promising application of VSC-HVDC to tackle, once and for all, severe instability problems or to improve system operation [26].

On the one hand, DC segmentation may seem to be going against the historical evolution of power systems as it consists in segmenting grids that have previously been linked together. However, it allows flexible control of the power exchanged between regions, while limiting the propagation of perturbations [27].

On the other hand, DC segmentation can be seen as a natural evolution of power systems. Indeed, in some interconnections initially done by AC transmission lines, new HVDC links have been built and, in some places, the latter are progressively taking over a large part of the total trans-border capacity. If the trend continues, in some specific situations one may ask why the AC transmission lines should be maintained, even if they transmit only a fraction of the power, while limiting the degrees of freedom of the system (as they force the two regions to stay in synchronism permanently). This situation has already occurred in southern China, where five HVDC links carry a total of 26 GW from Yunnan to Guangdong in parallel with AC lines. It has been found that a contingency of one of the DC links could lead to the overloading of the parallel inter-area AC lines and, since this risk was estimated to be more important than the service offered by the parallel AC lines, it was decided to disconnect them in July 2016; leading to the first documented DC segmentation of a power system [28].

Probably, the most extensively documented effect of DC segmentation is its ability to limit the propagation of perturbations across the different resulting clusters [27,29,30]. For example, [27] describes the HVDC links as “Grid Shock Absorbers” because, when controlled with constant power references, HVDC links are capable of preventing power or voltage fluctuations from propagating between different AC clusters, effectively serving as electrical firewalls. Thanks to this firewall effect, DC segmentation has the ability to reduce the risk of large-scale blackouts as illustrated in [31] with HVDC links controlled to provide frequency support, and in [32] with HVDC links emulating AC lines with a controllable impedance. Ref. [33] shows that DC segmentation can also be used to limit commutation failures of nearby LCC-HVDC converters. Thanks to the increase of controllability, market operation could become more efficient in a DC-segmented system, mainly if the segmentation boundaries separate different market sectors as illustrated in [27,34].

According to [25], DC segmentation could also increase the net transfer capacity between clusters, mainly because no line capacity needs to be held in reserve for uncontrolled power flows that can result from disturbances. Additionally, DC segmentation can result from the upgrading of existing HVAC lines to HVDC, which greatly increases their net transfer capacity [35,36].

Finally, regarding the impact of DC segmentation on power system stability, two main aspects, have been reported in the literature:

- DC segmentation can increase the angle stability margin of the system [37], since generators belonging to different clusters are not bond to stay in synchronism with one another, i.e., segmentation suppresses the synchronisation constraint between the AC clusters. In general, DC segmentation could improve angle stability under large disturbances (transient stability) and under small disturbances (electromechanical oscillations) [38].
- DC segmentation can jeopardise the frequency stability of the resulting asynchronous clusters, since each of the resulting cluster will have a smaller inertia and weaker frequency support than the original system [29,32].

Regarding electromechanical oscillations, the work in [39] analysed electromechanical oscillations in an AC power system segmented with LCC-HVDC links. The study shows that an increase of the load in the DC-segmented system reduces the damping ratio of some electromechanical modes and the work proposes an operating-point adjustment of the active-power flow of the LCC-HVDC segments to improve it. The work in [40] also analyses a DC-segmented system with LCC-HVDC links. It proposes two control strategies for the LCC-HVDC segments to improve the overall stability of the system, in terms of electromechanical oscillations. The control strategies consist in adding a supplementary set-point value to the DC-current reference of the rectifier station and a supplementary set-point value to the DC-voltage reference of the inverter station, which leads to an active-power modulation in the LCC-HVDC segments. The first control strategy (GSC1) should isolate the electromechanical oscillations in each asynchronous area. The second control strategy (GSC2) allows the propagation of electromechanical oscillations among the asynchronous AC areas of the DC-segmented system, but should improve the overall small-signal angle stability. The work in [38] presented a comprehensive analysis of the impact of DC segmentation on transient stability, electromechanical-oscillation damping and frequency stability in power systems. It showed that DC segmentation, where VSC-HVDC systems are controlled with constant-power set points, could improve transient stability and the damping of (even suppress) electromechanical oscillations (i.e., DC segments as firewalls), although the overall frequency stability may deteriorate, because the inertia and primary frequency support of the resulting asynchronous AC clusters will be reduced. More recently [24] proposed an algorithm to automatically obtain a DC-segmentation solution for a given AC power system with the purpose of mitigating electromechanical oscillations by suppressing dangerous inter-area oscillation modes, using VSC-HVDC links. Since in [24] the VSC-HVDC links used where controlled with constant active- (P) and reactive-power (Q) injections, there is still room for further improvements to take full advantage of an expensive and permanent solution such as DC segmentation. In fact, once an inter-area oscillation mode has been eliminated (as in [24]), the following questions may arise:

- Could the damping ratio of the intra-area electromechanical modes of the remaining AC clusters be increased?
- Could the overall frequency stability of the resulting DC-segmented system be improved?

Along these lines, the contributions of this paper are as follows:

- Investigation of the use of supplementary reactive-power controllers in the VSC-HVDC systems of a DC-segmented system to damp intra-area oscillations in the remaining AC clusters (POD-Q controllers, for short). Two POD-Q controllers are analysed: (a) one using local frequency as input signal (based on previous proposals in the literature) and (b) another one using the frequency of the Centre Of Inertia (COI) of each AC cluster, which is a new proposal of this work.
- Investigation of the use of supplementary active-power/frequency controllers (FCs) in the VSC-HVDC converters of a DC-segmented system to improve frequency stability.

The use of Q control to tackle intra-area oscillation damping while P control is used for frequency support is motivated by the following reasons.

1. Active-power control: Frequency support among asynchronous AC systems through VSC-HVDC can be applied directly, as shown in previous work. However, although active-power control is an attractive alternative for power-oscillation damping (POD-P) in VSC-HVDC systems embedded in AC systems, the use of POD-P controllers in VSC-HVDC interconnecting asynchronous AC systems is not trivial at all. This is due to the fact that one converter station would be modulating its active-power injection to damp electromechanical oscillations in one AC area, but it would also be including a continuous perturbation into the other asynchronous AC area.
2. Reactive-power control: Due to the independent control in VSC stations, Q modulation (POD-Q) in converter stations could be used to damp intra-area oscillations in VSC-HVDC systems interconnecting asynchronous AC grids, without propagating perturbations among those grids due to the control actions.
3. Since P control is used for frequency support and Q control for power-oscillation damping, both applications could be used simultaneously in the context of VSC-HVDC interconnecting AC grids without interaction, as shown in the paper.

Notice that, although POD controllers [15] and frequency controllers [41–43] in VSC-HVDC systems have been analysed in previous work, the work reported here has explored their application to a DC-segmented system and results show that both controllers can be applied with no significant interaction between them, and without jeopardising the solution for the original problem DC segmentation was intended for.

2. DC segmentation of power systems and VSC-HVDC systems

Fig. 1-a shows a schematic diagram of an AC power system and Fig. 1-b shows the power system after DC segmentation, where an AC line has been replaced by a VSC-HVDC link, decoupling the two remaining AC systems. Notice that, in general, a DC-segmented system may need more than one VSC-HVDC link to decouple the asynchronous AC clusters of the system.

As mentioned before, the determination of the most appropriate locations of the decoupling DC links (VSC-HVDC) to mitigate a critical inter-area oscillation mode of the original AC system, without impacting on the local electromechanical modes of the asynchronous clusters, was addressed in [24]. That reference uses the concept of electromechanical-oscillation path proposed in [44] and assumes constant-power control of the VSC-HVDC links. The present work goes a step further as it will consider supplementary controllers on the converter stations (a) to damp intra-area oscillations in the asynchronous AC clusters and (b) to provide frequency support among the asynchronous AC clusters, as it will be described in Section 3.

For this study, electromechanical-type models of VSC-HVDC systems, also known as Root-Mean-Square (RMS) models, are used, following the guidelines of [45], as illustrated in Fig. 2. Every VSC station is modelled as a voltage source at its AC side ($E_m \angle \theta_m$) connected to the rest of the system by a series impedance that aggregates the AC reactor and the transformer (L_{eq}^{ac}, R_{eq}^{ac}). Meanwhile, VSC stations are seen as current injections at their DC side (I_{dc}). AC and DC sides are coupled by the energy conservation principle:

$$P_m + P_{dc} + P_{loss} = 0 \tag{1}$$

where P_{dc} is the input active power injected in the DC link, P_m is the active power injected in the AC side and P_{loss} are the losses in the converter station. For simplicity, P_{loss} has been neglected in the work reported here. A typical way in which P_{loss} can be taken into account is explained in [46], where a quadratic function of the RMS value of the converter AC current is used. Ref. [46] also gives the parameters for the loss function derived from an actual installation.

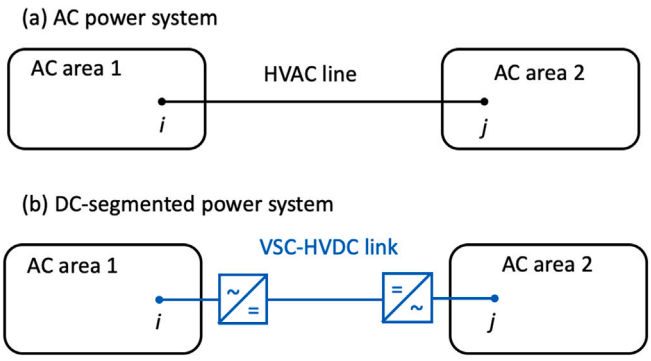

Fig. 1. (a) AC power system and (b) DC-segmented power system.

VSC stations are controlled with conventional Grid-Following (GFL) vector control and the model includes their operation limits, as described in [45]. In each VSC-HVDC link, one VSC station controls its active-power injection, while the other one controls the DC voltage. Meanwhile, each VSC station controls its reactive power injection independently. Finally, the DC grid is represented with the equivalent capacitor at each DC bus (C_{eq}^{dc}) and with the series resistances and inductances of the DC lines.

3. Supplementary controllers for VSC stations

The following supplementary controllers in the VSC-HVDC links of the DC-segmented system will be considered:

- Frequency Controllers (FCs): Their objective is to provide frequency support between the asynchronous AC areas through the VSC-HVDC links.
- Power-Oscillation Damping (POD) controllers applied to Q injections (POD-Q): Their objective is to contribute to damp intra-area oscillations in the asynchronous AC areas by means of Q-modulation in the VSC stations of the DC segments.

3.1. Frequency controllers (FCs)

In FCs, the P set point of the VSC station that controls the active power through each DC segment (VSC-i) is given by:

$$P_{ac,i}^{*} = P_{ac,i}^{0} + \Delta P_{ac,i}^{ref,FC} \tag{2}$$

where $P_{ac,i}^{0}$ is a constant P set-point value, and $\Delta P_{ac,i}^{ref,FC}$ is the supplementary P set-point value provided by the FC.

Fig. 3 shows the block diagram of a FC proposed in [42] for each converter (i) in a "multiterminal HVDC system with VSC technology" (VSC-MTDC). It uses the average output frequency of the converter stations in the VSC-MTDC system as the set point ($\omega^{*} = \bar{\omega}$). In each converter, it includes a proportional controller with gain $K_{FC,i}$, a low-pass filter with time constant $T_{FC,i}$ and a saturation parameter $\pm\Delta P_{ac,i}^{max}$ and will be referred to as FC-WAF in the rest of the paper. When applied to a two-terminal DC link, the frequency set point for the FC in each converter is given by:

$$\omega^{*} = \bar{\omega} = \frac{\omega_i + \omega_j}{2} \tag{3}$$

where ω_i and ω_j are the frequencies measured at the two AC terminals of the VSC-HVDC link (in pu).

Notice that in point-to-point VSC-HVDC links, strategy FC-WAF [42] is equivalent to a proportional FC applied to the frequency difference between the two terminals of the link, as long as $K'_{FC,i} = K_{FC,i}/2$:

$$\Delta P_{ac,i}^{ref,FC} = \frac{K_{FC,i}}{1 + sT_{FC,i}}(\bar{\omega} - \omega_i) \tag{4}$$

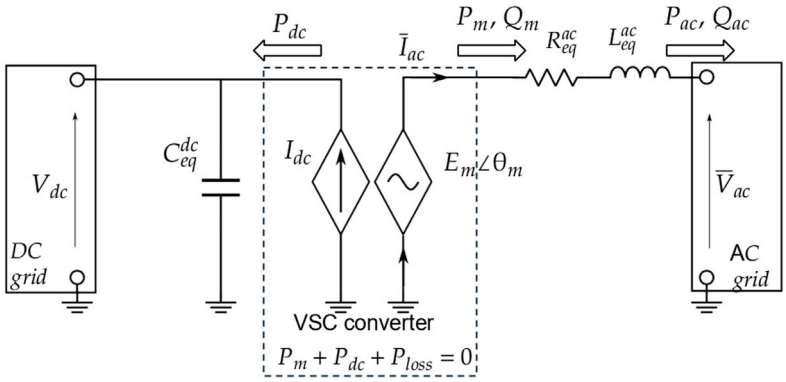

Fig. 2. Model of a VSC station.

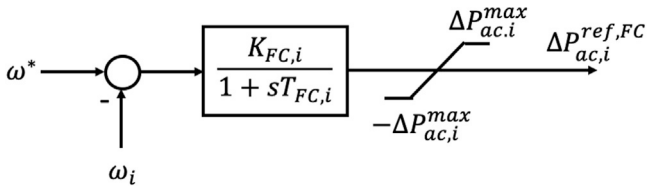

Fig. 3. Schematics for a FC-WAF controller for a VSC station.

$$= \frac{K_{FC,i}}{1+sT_{FC,i}}\left[\frac{\omega_i+\omega_j}{2}-\omega_i\right]$$
$$= \frac{K_{FC,i}/2}{1+sT_{FC,i}}(\omega_j-\omega_i) = \frac{K'_{FC,i}}{1+sT_{FC,i}}(\omega_j-\omega_i).$$

With the FC-WAF of Fig. 3, frequency support among the asynchronous AC areas through the VSC-HVDC links is achieved, independently of the location of the disturbance, since the FC-WAF uses frequency measurements at both ends of the VSC-HVDC links.

3.2. POD-Q controllers

This section will illustrate whether the control of the reactive power (Q) injected by the VSCs of the HVDC links used for the DC segmentation of an AC system can improve the damping of power oscillations within the resulting AC sections (Power-Oscillation Damping using Q or POD-Q).

Let us assume that the Q injected by a VSC-i into the AC system is modulated around its operating point as follows:

$$Q_{ac,i}^{*} = Q_{ac,i}^{0} + \Delta Q_{ac,i}^{ref,POD} \tag{5}$$

where $Q_{ac,i}^{*}$ is the Q set point, $Q_{ac,i}^{0}$ is a constant Q set-point value applied in the operating point if power oscillations were not present, and $\Delta Q_{ac,i}^{ref,POD}$ is the supplementary Q set-point value provided by a POD-Q controller to tackle power oscillations.

Two POD-Q controllers for the VSC stations (POD-Q) will be analysed and compared in this work:

- POD-Q-LF: It modulates the Q injections of each VSC-i using local measurement of the frequency at the AC connection point of the VSC.
- POD-Q-FCOI: It modulates Q injections of each VSC-i using both local measurement of the frequency at the AC connection point of the VSC and global measurements of the frequency of the Centre Of Inertia (COI) of the AC area to which the VSC is connected.

The two POD-Q controllers above can be described with the scheme of Fig. 4. The input signal of the controller is the frequency error (in pu) between the frequency set point (ω_i^*) and the frequency measured at the AC connection point of each VSC-i station (ω_i). The POD-Q controller has a low-pass filter (with time constant $T_{Qf,i}$), a wash-out filter (with time constant $T_{QW,i}$), $N_{QS,i}$ lead/lag filters (with time constants $T_{Q1,i}$, $T_{Q2,i} = a_{Q,i}T_{Q1,i}$, i.e., a filtering ratio $a_{Q,i}$), a controller gain $K_{Q,i}$ and a saturation parameter $\pm\Delta Q_{ac,i}^{max}$.

3.2.1. POD-Q-LF

In a POD-Q-LF controller, the frequency set point of Fig. 4 is the nominal frequency in pu: $\omega_i^* = \omega_0 = 1$ pu. Hence, it only uses local measurements (ω_i). This scheme of POD-Q controller is based on previous proposals in the literature [10,47].

3.2.2. POD-Q-FCOI

In POD-Q-FCOI controller, newly proposed in this work, the frequency set point of Fig. 4 is calculated as the frequency of the COI (in pu) of the AC area in which station VSC-i is connected:

$$\omega_i^* = \omega_{COI,i} = \sum_{k\in A_i}\frac{H_k}{H_T}\omega_k,\ H_T = \sum_{j\in A_i} H_j. \tag{6}$$

This strategy was motivated by a proposal in [16] for VSC-MTDC systems embedded in an AC system, which used the weighted-average output frequency of the converters in the VSC-MTDC system as frequency set point. However, here the VSC-HVDCs are interconnecting asynchronous AC areas, and each VSC-i need not know the output frequency of the other VSCs. In POD-Q-FCOI controller, each VSC compares the frequency set point with $\omega_i^* = \omega_{COI,i}$ with its own frequency (ω_i). The usefulness of the speed of the COI for power-system-stability-tailored controllers was already illustrated in [48].

3.3. Design of POD-Q controllers

The design procedure used for POD-Q controllers is based on the work in [11], which uses the concept of eigenvalue sensitivities [49]. The work in [16] already used this approach for the design of POD controllers in VSC-HVDC systems. In the work described here, eigenvalue sensitivities have been calculated numerically (i.e. using finite differences), as it can facilitate the design of POD controllers in cases with limited information of the state matrices of the linearised system.

Let us assume that a linearised model of the power system is available and there exist a lightly damped electromechanical mode i that will be targeted by the design:

$$\lambda_i^0 = \sigma_i^0 \pm j\omega_i^0 \tag{7}$$

If the damping ratio of the targeted electromechanical mode of the original system is called ζ_i^0 and the required damping ratio is called ζ_i^d, the resulting electromechanical mode, after compensation, can be approximated as:

$$\lambda_i^d = -\zeta_i^d\omega_i^0 \pm j\omega_i^0 \tag{8}$$

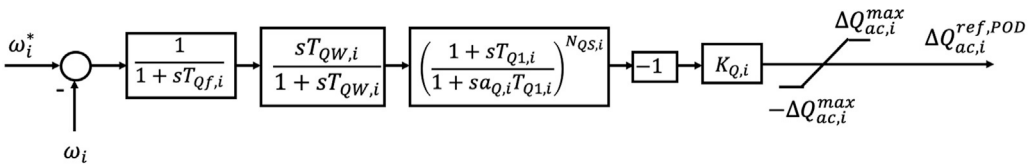

Fig. 4. A general POD-Q controller.

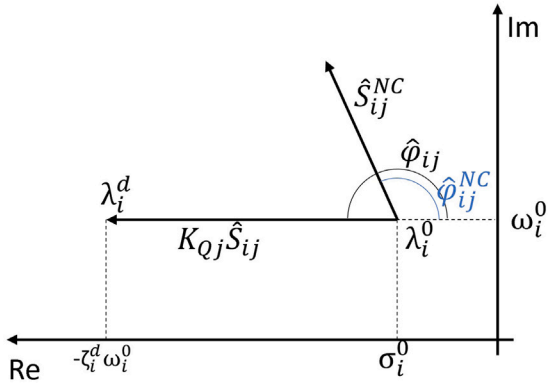

Fig. 5. Geometric interpretation of eigenvalue sensitivities.

The sensitivity of electromechanical mode i to changes in the gain of POD-Q controller j, $K_{Q,j}$, is defined as [49]:

$$S_{ij} = \frac{\partial \lambda_i}{\partial K_{Q,j}} \tag{9}$$

Similarly, the sensitivity of mode i to changes in the gain of the non-compensated ($T_{Q1,j} = 0$ in the lead/lag compensator) POD-Q controller j (S_{ij}^{NC}) is:

$$\begin{aligned} S_{ij}^{NC} &= S_{ij}(T_{Q1,j} = 0) = \left.\frac{\partial \lambda_i}{\partial K_{Q,j}}\right|_{T_{Q1,j}=0} \\ &= |S_{ij}^{NC}| \angle \varphi_{ij}^{NC} \end{aligned} \tag{10}$$

S_{ij}^{NC} in (10) can be approximated using finite differences as:

$$\hat{S}_{ij}^{NC} = \frac{\lambda_i^{NC} - \lambda_i^0}{\Delta K_{Q,j}} \tag{11}$$

where λ_i^{NC} is the non-compensated eigenvalue, i.e., the new eigenvalue with the POD-Q implemented without its lead/lag compensator ($T_{Q1,j=0}$), and with a small gain change $\Delta K_{Q,j}$.

Fig. 5 shows the geometric interpretation of eigenvalue sensitivities [11,16]. An effective POD-Q will move the targeted electromechanical mode to the left-hand side of the complex plane, as illustrated in Fig. 5. The lead/lag compensator is used to ensure that the eigenvalue sensitivity has phase as close to 180° as possible, while gain $K_{Q,j}$ (see Fig. 4) is used to move the eigenvalues further to the left-hand side of the complex plane and to achieve the required damping ratio.

The design of the POD-Q controller of each VSC-j consists of two steps [11]:

1. *Design of the lead/lag compensator:* Its objective is to obtain a phase of the eigenvalue sensitivity ($\hat{S}_{ij}$) as close to 180° as possible:

   - If a phase lead ($\hat{\varphi}_{ij}^{NC} \geq 0$) is required:

   $$a_{Q,j} = \frac{1 - \sin\phi_{ij}}{1 + \sin\phi_{ij}} \leq 1, \ \phi_{ij} = \frac{\pi - \hat{\varphi}_{ij}^{NC}}{N_{QS,j}}. \tag{12}$$

   - If a phase lag is required ($\hat{\varphi}_{ij}^{NC} < 0$) is required:

   $$a_{Q,j} = \frac{1 + \sin\phi_{ij}}{1 - \sin\phi_{ij}} > 1, \ \phi_{ij} = \frac{\pi + \hat{\varphi}_{ij}^{NC}}{N_{QS,j}}. \tag{13}$$

   with $\hat{\varphi}_{ij}^{NC} = \angle(\hat{S}_{ij}^{NC})$. In addition, time constant $T_{Q1,j}$ of the lead/lag compensator is selected to achieve maximum lead/lag phase compensation at the frequency of the targeted electromechanical mode [50]. Therefore:

   $$T_{Q1,j} = \frac{1}{\omega_i^0 \sqrt{a_{Q,j}}}, \text{ and } T_{Q2,j} = a_{Q,j} T_{Q1,j}. \tag{14}$$

   The resulting numerical eigenvalue sensitivity can be then calculated as:

   $$\hat{S}_{ij} = \hat{S}_{ij}^{NC} \left[\frac{1 + sT_{Q1,j}}{1 + sa_{Q,j}T_{Q1,j}}\right]^{N_{QS,j}}_{s=\lambda_i^0} = |\hat{S}_{ij}^{NC}| \angle \hat{\varphi}_{ij} \tag{15}$$

2. *Calculation of the controller gain:* Gain $K_{Q,j}$ is calculated to obtain the required damping ratio of the targeted electromechanical mode:

   $$\lambda_i^d \approx \lambda_i^0 + K_{Q,j}\hat{S}_{ij}. \tag{16}$$

   $$K_{Q,j} = \gamma_j \frac{|\lambda_i^d - \lambda_i^0|}{|\hat{S}_{ij}|} \tag{17}$$

   with $K_{Q,j} \in [-K_{Q,j}^{max}, K_{Q,j}^{max}]$, and $\gamma_j = 1$ if a positive gain is required and $\gamma_j = -1$ if a negative gain is required.

4. Case study and results

The Nordic 44 AC test system [51] has been used to analyse DC segmentation with the supplementary controllers described in Section 3. The Nordic 44 test system was initially implemented within the iTesla project as an application example of the OpenIPSL library, implemented in the Modelica language [52,53]. The version used in this paper is the one updated by the ALSETlab. The simulations will be carried out using the Dymola environment. OpenIPSL can be used for non-linear electromechanical time-domain simulation, and small-signal stability analysis. The information about the scenario considered is provided in Appendix A.1 of Appendix A.

The starting point for the work presented in this paper is the architecture for DC-segmentation shown in Fig. 6 resulting from the algorithm tailored to the mitigation of electromechanical oscillations proposed in [24]. VSC-HVDC link A has a rating of 3500 MVA, while VSC-HVDC link B has a rating of 800 MVA. Supplementary controllers for frequency support between the two AC areas (FC) and power-oscillation damping for the intra-area modes by means of Q-modulation at the VSC stations (POD-Q controllers) will now be analysed (see Section 3).

Four cases will be analysed and compared:

- **AC base case**: The initial Nordic 44 test system. It corresponds to the case of Fig. 6 with AC lines instead of the DC links.
- **DCs constant PQ**: The DC-segmented case without supplementary controllers.
- **DCs f-support, POD-Q-LF**: The DC-segmented case with frequency support (FC) and POD-Q using local frequency (POD-Q-LF).

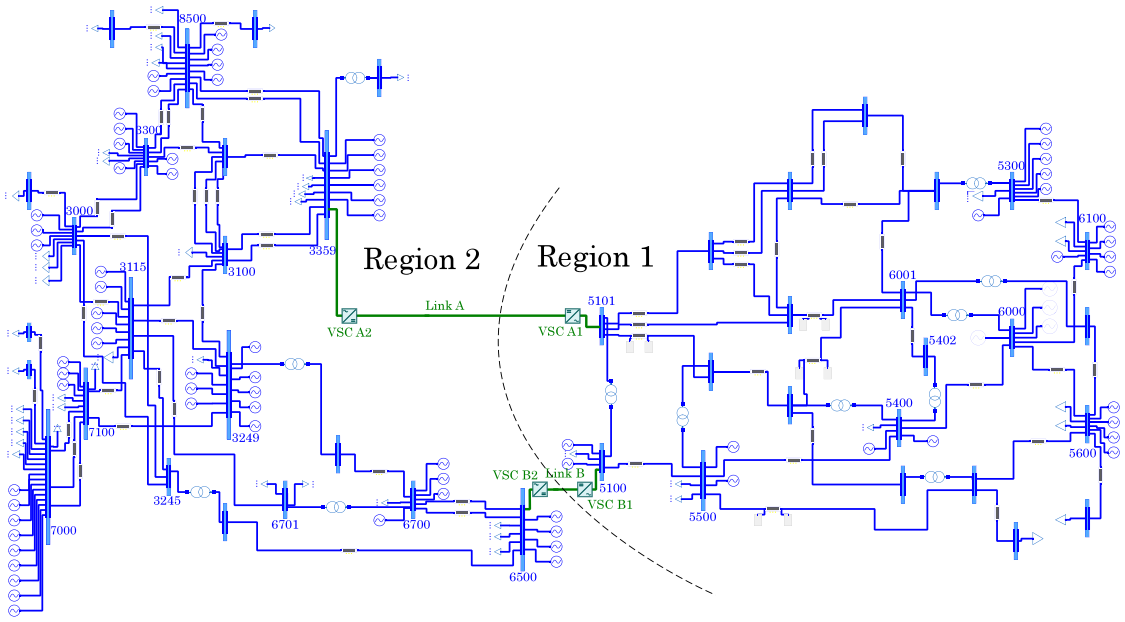

Fig. 6. DC-segmented N44 test system under Dymola.

- **DCs f-support, POD-Q-FCOI**: The DC-segmented case with frequency support (FC) and POD-Q using the frequency of the centre of inertia of each AC area (POD-Q-FCOI).

In the two cases with supplementary controllers (DCs f-support, POD-Q-LF and DCs f-support, POD-Q-FCOI), both f-support and POD-Q are implemented in the four VSCs. Additional information about the VSCs is provided in Appendix A.2.

In the operating point, the power flows through the VSC-HVDC links are the same as the power flows through the AC lines of the base case: 447 MW and 1548 MW (from Region 1 to Region 2). The four cases have been compared by means of small-signal stability analysis (see Section 4.2) and non-linear time-domain simulations (see Section 4.3).

4.1. Design of POD-Q controllers

Table 1 includes the modes of interest of the Nordic 44 test system in the AC case and in the DC-segmented case without supplementary controllers. All the electromechanical modes with a damping lower than 20% in at least one of the cases have been included. The table also indicates the location of each mode. Results show that the critical inter-area mode (mode 1), which had a low damping ratio in the original AC system, has been eliminated with the DC-segmentation architecture obtained with the algorithm proposed in [24]. Nevertheless, there are still worrying intra-area modes in each asynchronous AC area. POD-Q controllers (POD-Q-LF and POD-Q-FCOI described in Section 3.2) will be used at every VSC station to increase the damping ratio of some intra-area modes. POD-Q controllers will be designed following the methodology presented in Section 3.3.

POD-Q controllers of VSCs of region 1 (ie. VSC-A1 at bus 5101 and VSC-B1 at 5100) target mode 2 (with a damping ratio of $\zeta = 5.7$ % and a frequency of 0.80 Hz) while the VSC of region 2 (ie. VSC-A2 at bus 3359 and VSC-B2 at bus 6500) targets mode 4 (with a damping ratio of $\zeta = 11.92$ % and a frequency of 0.72 Hz). Each POD-Q controller has been designed independently to obtain a 15 % damping for the targeted mode. The Gain step used for the calculation of the numerical eigenvalue sensitivity was $\Delta K_{Q,j} = 20$ pu (nominal pu). Pre-defined parameters of the POD-Q controllers are: $T_{Qf,j} = 0.1$ s, $T_{QW,j} = 5$ s, $N_{QS,j} = 2$ and $\pm\Delta Q_{ac,i}^{max} = \pm 0.1$ pu. Maximum allowed POD-Q gain was set to $K_{Q,j}^{max} = \pm 400$ pu. Notice that $K_{Q,j}^{max}$ must be limited so that (a) a linear approximation to the eigenvalue behaviour can be trusted and (b) undesirable behaviour, such as stability issues or reaching operating limits too often during transients, is avoided. Before taking any decision, the final position of the targeted eigenvalue must be double-checked. Notice that a range of $[-400, 400]$ pu in POD controller gain is consistent with parameters used in previous work on POD-P and POD-Q controllers in VSC-HVDC systems when using frequency-related input signals [16,54,55].

Table 1
Poorly-damped electromechanical modes of the two initial cases.

N0.	AC base case		DCs constant PQ		Region of
	ζ (%)	Freq. (Hz)	ζ (%)	Freq. (Hz)	the mode
1	1.85	0.39	–	–	Inter-area
2	5.45	0.83	5.70	0.80	R1
3	11.68	0.88	11.92	0.87	R2
4	12.11	0.75	11.73	0.72	R2
5	–	–	12.06	1.12	R2
6	12.12	1.07	12.14	1.07	R1
7	12.22	0.54	12.38	0.50	R2
8	13.12	0.98	13.12	0.95	R2
9	13.57	1.23	17.37	1.27	R1
10	15.69	1.10	14.81	1.12	R1

Table 2
Parameters of the POD-Q controllers.

Case	VSC	$K_{Q,j}$ (pu)	$T_{Q1,j}$ (s)	$a_{Q,j}$
POD-Q-LF	A1 (5101)	−400	0.2847	0.486
	B1 (5100)	−400	0.2847	0.486
	A2 (3359)	400	0.2223	0.999
	B2 (6500)	400	0.2975	0.558
POD-Q-FCOI	A1 (5101)	−400	0.2750	0.521
	B1 (5100)	−400	0.2776	0.511
	A2 (3359)	400	0.2402	0.856
	B2 (6500)	400	0.2889	0.592

Table 2 shows the parameters obtained for POD-Q-LF (local) and POD-Q-FCOI (global) controllers with the design procedure described in Section 3.3. Notice that POD-Q gains reach their maximum allowed value. This is due to the fact that POD controllers in VSC-HVDC systems are only really effective if the VSC stations are well located to damp electromechanical oscillations [16]. However, POD-Q controllers in a DC-segmented system may not be in the best location to damp

Table 3
Poorly-damped electromechanical modes of the four scenarios considered.

N0.	AC base case		DCs constant PQ		DCs f-support POD-Q-LF		DCs f-support POD-Q-FCOI		Region of
	ζ (%)	Freq. (Hz)	ζ (%)	Freq. (Hz)	ζ (%)	Freq. (Hz)	ζ (%)	Freq. (Hz)	the mode
1	1.85	0.39	–	–	–	–	–	–	Inter-area
2	5.45	0.83	5.70	0.80	11.53	0.84	12.40	0.83	R1
3	11.68	0.88	11.92	0.87	12.30	0.88	12.33	0.88	R2
4	12.11	0.75	11.73	0.72	15.52	0.74	15.40	0.74	R2
5	–	–	12.06	1.12	12.44	1.10	12.16	1.07	R2
6	12.12	1.07	12.14	1.07	12.15	1.07	12.48	1.10	R1
7	12.22	0.54	12.38	0.50	15.02	0.48	16.45	0.47	R2
8	13.12	0.98	13.12	0.95	16.05	0.97	15.61	0.97	R2
9	13.57	1.23	17.37	1.27	20.68	1.31	20.68	1.31	R1
10	15.69	1.10	14.81	1.12	14.30	1.21	14.55	1.20	R1

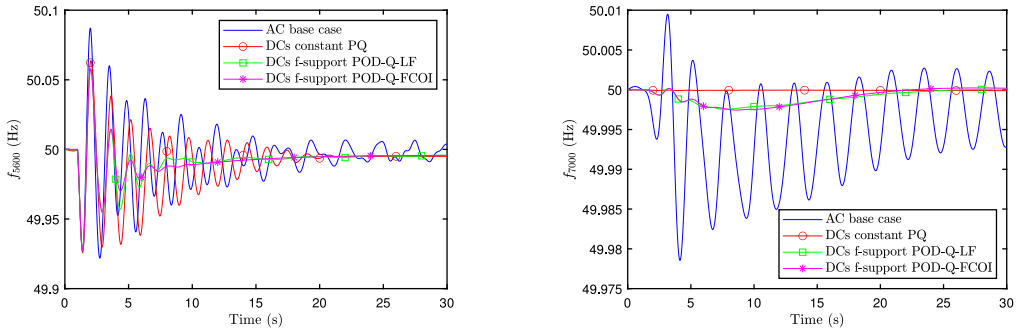

(a) Region 1 (b) Region 2

Fig. 7. Frequency of two representative generators after the disconnection of line 6001-5301 (Region 1).

electromechanical oscillations. Precisely, the aim of this work is to analyse the capability of damping intra-area electromechanical modes in DC-segmented system with a pre-defined scheme. It is also worth mentioning that some POD-Q gains have opposite signs, which is also related to the location of the VSC stations in each AC area.

4.2. Small-signal stability analysis

Table 3 shows the most important electromechanical modes of the system for the 4 cases.

Results show that:

- The inter-area mode (mode 1 with a damping ratio of 1.85% and a frequency of 0.39 Hz) has been suppressed by the DC segmentation.
- The damping of the main intra-area mode of region 1 (mode 2 with a damping ratio of 5.7% and a frequency of 0.8 Hz in the DC-segmented case without control) has been improved by the POD-Q controllers (+5.97% with POD-Q-LF and +7.04% with POD-Q-FCOI).
- The damping of the main intra-area mode of region 2 (mode 4 with a damping ratio of 11.73% and a frequency of 0.72HZ in the DC-segmented case without control) has been improved by the POD-Q controllers (+3.62% with POD-Q-LF and +3.67% with POD-Q-FCOI).
- Meanwhile, the damping ratios of the rest of the electromechanical modes do not change significantly.

Notice that in the DC-segmented case, results obtained with POD-Q-FCOI (global measurements) are only slightly better than the ones obtained with POD-Q-LF (local measurements). Therefore, taking into account that the implementation of local measurements is much easier, for this test system the use of POD-Q-LF seems to be a better solution than POD-Q-FCOI.

4.3. Non-linear time-domain simulation

4.3.1. Small perturbation

The disconnection of line 6001-5301 at Region 1 at $t = 1$ s (a small perturbation) has been simulated to analyse electromechanical oscillations.

Fig. 7 shows the frequency of two representative generators (5600 in Region 1 and 7000 in Region 2) and Fig. 8 shows the Q injections of the VSCs of Region 1 after the disconnection of the line in Region 1. A poorly-damped inter-area oscillation can be clearly observed in the AC base case, which corresponds to mode 1 of Table 3 (see Fig. 7). Results confirm the suppression of the inter-area mode in the 3 DC-segmented cases and the improvement of the first local mode of Region 1 (mode 2 of the Table 3) in the two DC-segmented cases with both POD-Q-LF and POD-Q-FCOI. POD-Q-LF and POD-Q-FCOI controllers damp intra-area oscillations successfully (see Fig. 7(a) by means of reactive-power modulation (Fig. 8). Notice that in the DC-segmented case with constant power control, the perturbation that occurs at Region 1 is not propagated to Region 2 and the frequency at buses in Region 2 remain equal to 50 Hz (see Fig. 7(b)). On the contrary, a small transient on the frequency at Region 2 is observed in the DC-segmented cases with supplementary controllers. This is due to the effect of the frequency controllers placed in the VSC-HVDC links.

4.3.2. Disconnection of a generator

The disconnection of a generator at bus 5300 (G5300-1 at Region 1) at $t = 1$s has been simulated. This generator has a nominal power of 1200 MVA and was injecting 723 MW before the event, making it the generator with the highest active-power injection at that time. The purpose of this simulation is to analyse frequency stability.

Fig. 9 shows the frequency of the two representative generators used above after the disconnection of the generator in Region 1, while Fig. 10 shows the active power exchange between the two regions (from Region 1 to Region 2). In the AC base case, the frequency nadir and the

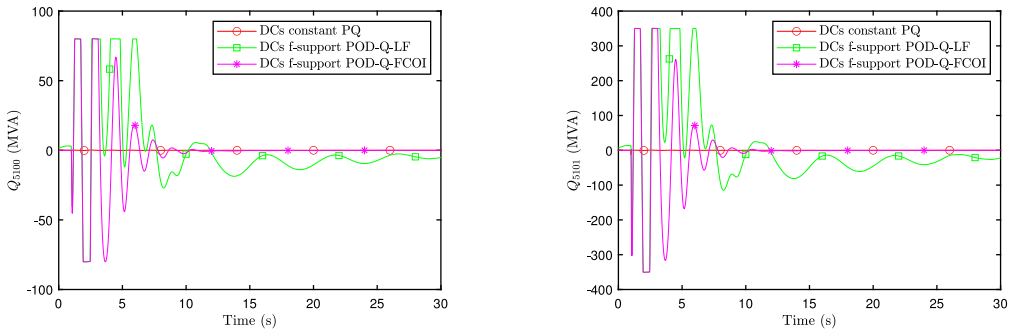

(a) VSC A1 (5100) (b) VSC B1 (5101)

Fig. 8. Reactive power injections at the two VSCs of Region 1 after the disconnection of line 6001-5301 (Region 1).

Table 4
Frequency Nadir and steady state after a disconnection of generator in Region 1 or 2 in the four cases.

Disconnection of generator in:	Frequency (Hz)	AC case	DCs constant PQ	DCs f-support POD-Q-LF	DCs f-support POD-Q-FCOI
Region 1	f_{min} (Hz)	49.85	49.68	49.74	49.75
	f_{final} (Hz)	49.97	49.94	49.94	49.94
Region 2	f_{min} (Hz)	49.86	49.76	49.79	49.79
	f_{final} (Hz)	49.97	49.93	49.94	49.94

final frequency are lower than the ones obtained in Region 1 of the DC-segmented case, because the two areas are connected synchronously through AC branches and there is a better total frequency-support capability. Naturally, in the AC base case the frequencies at regions 1 and 2 are in synchronism. In the DC-segmented case with constant power control, the frequency nadir in Region 1 is very low because this region only has frequency support from its synchronous generators as the VSC-HVDC links do not provide frequency support. Furthermore, in the case of DC segmentation with constant power, the frequency at Region 2 remains constant, because it is decoupled from Region 1 by the VSC-HVDC links. On the contrary, in the DC-segmented cases with supplementary controllers, FCs in the VSC-HVDC links produce frequency support between the two regions, and the frequency nadir is higher than in the case without supplementary controllers. The effects of frequency support through the VSC-HVDC links can be better observed in Fig. 10, where they reduce the power exchange between Regions 1 and 2. As a consequence, in the DC-segmented cases with supplementary controllers, the frequency at Region 2 also changes.

Table 4 shows the frequency nadir (f_{min}) and final steady-state frequency (f_{final}) after the disconnection of generator G5300-1 in Region 1. Note that the results of the table may not correspond exactly to the ones of Fig. 9 for the final frequency since the steady state has not been reached in the figure. Results for the disconnection of a generator in Region 2 are also included in the table (G3300-1). The chosen generator has a nominal power of 1100 MVA and was injecting 757 MW before the event. As a conclusion, in the DC-segmented cases with supplementary controllers, overall frequency stability is improved, in comparison with the DC-segmented case with constant power.

Additionally, DC segmentation with and without frequency support significantly reduces the change of power flow in the inter area link (see Fig. 10). This could avoid tripping of the line in cases where the link is close to its maximum capacity.

4.4. Impact of communication latency

The implementation of the POD-Q-FCOI requires a communication system between the generators and the VSCs and its impact on the performance of the controller is analysed here.

Table 5
Poorly-damped electromechanical modes with POD-Q-FCOI control for frequency support, and various communication delays.

N0.	No delay		τ = 0.05 s		τ = 0.1 s		Region of
	ζ (%)	Freq. (Hz)	ζ (%)	Freq. (Hz)	ζ (%)	Freq. (Hz)	the mode
2	12.40	0.83	11.14	0.84	9.95	0.84	R1
3	12.33	0.88	12.19	0.88	12.04	0.88	R2
4	15.40	0.74	14.86	0.74	14.37	0.75	R2
5	12.16	1.07	12.19	1.07	12.22	1.07	R2
6	12.48	1.10	12.65	1.10	12.79	1.10	R1
7	16.45	0.47	17.41	0.48	18.28	0.48	R2
8	15.61	0.97	15.10	0.98	14.11	0.99	R2
9	20.68	1.31	20.68	1.31	20.68	1.31	R1
10	14.55	1.20	13.84	1.20	13.18	1.19	R1

Assuming a central control scheme, the input error signal of POD-Q-FCOI of Fig. 4 with a communication delay may be written as:

$$u_i = e^{-s\tau}(\omega_{COI,i} - \omega_i) \tag{18}$$

where τ is the total communication delay.

The delay of (18) was implemented using a first-order Padé's approximation and realistic values of communication latency delays were analysed (τ = 50 ms and τ = 100 ms).

Table 5 shows the main electromechanical modes of the system for different values of communication delays when POD-Q-FCOI for frequency support was used . The modes considered are the same as the ones of Table 3. Results show that the communication delays slightly reduce the damping ratio of the target modes (from 12.40% to 9.95% for mode 2 and from 15.40% to 14.37% for a delay τ = 0.1 s) without significant impact on other modes. Therefore, results prove that a POD-Q-FCOI controller is robust against communication latency. Independently of this, as previously discussed, since a POD-Q-LF controller uses only local signals and both controllers produce similar results, a POD-Q-LF controller appears to be a better alternative than POD-Q-FCOI control, at least for the test system used in this work.

5. Conclusions

The conclusions of the work presented here can be summarised as follows:

- DC segmentation can be very effective to suppress critical inter-area oscillation in stressed AC power systems. However, if VSC-HVDC systems are controlled with constant power: (a) overall frequency stability may deteriorate greatly, because each asynchronous AC cluster will have lower amounts of frequency support and inertia and (b) intra-area electromechanical oscillations in the AC clusters may have similar damping ratio to those obtained in the AC base case.

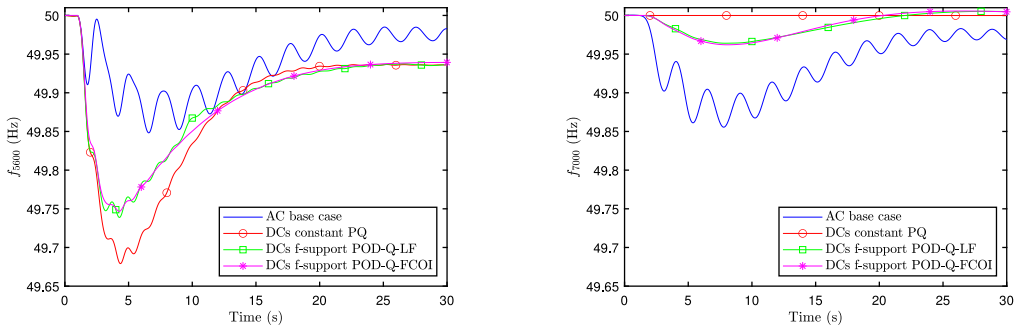

(a) Region 1 (b) Region 2

Fig. 9. Frequency of two representative generators after the disconnection of a generator at bus 5300 (Region 1).

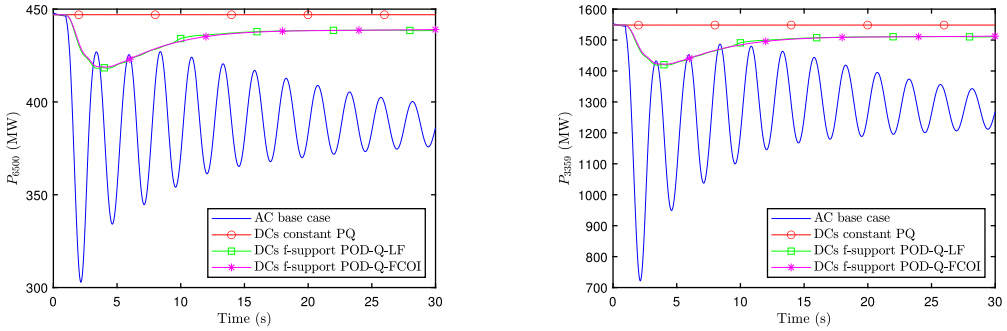

(a) Link A (5100-6500) (b) Link B (5101-3359)

Fig. 10. Active power exchange from region 1 to region 2 after the disconnection of a generator at bus 5300 (Region 1).

- Frequency controllers (FC) in the VSC-HVDC links of a DC-segmented system can provide frequency support between the different AC clusters, improving overall frequency stability, in comparison with DC segmentation with constant power control.
- Power-oscillation damping controllers for the reactive-power injections (POD-Q) in the VSC-HVDC links of a DC-segmented system can be used to damp intra-area oscillations of the asynchronous AC clusters, in addition to the mitigation of the critical inter-area oscillation due to DC segmentation. Two effective POD-Q controllers were analysed and compared: POD-Q-LF (using local measurements), based on previous proposals and POD-Q-FCOI (using global measurements), newly proposed in this work.
- POD-Q-LF (local) and POD-Q-FCOI (global) controllers produced comparable results, and the latter proved to be robust when subjected to communication delays. Nevertheless, considering that the implementation of POD controllers using remote signals is more complex and expensive than POD controllers using local signals only, POD-Q-LF controller seems to be a more practical solution than POD-Q-FCOI controller, at least for the test system considered.
- Eigenvalue sensitivities have been calculated numerically for the design of POD-Q controllers in the DC-segmented power system, which is only an approximation but can facilitate its implementation in small-signal-stability tools with limited information of the state matrices.
- The use of DC segmentation, frequency support and POD-Q control brought an important improvement of the overall stability of the test system compared to the initial AC case.
- Future work should investigate POD controllers and frequency controllers in DC-segmented power systems considering different scenarios.

CRediT authorship contribution statement

M. Robin: Writing – review & editing, Writing – original draft, Software, Methodology, Investigation, Formal analysis, Data curation, Conceptualization. **J. Renedo:** Writing – review & editing, Writing – original draft, Validation, Supervision, Software, Project administration, Methodology, Investigation, Formal analysis, Data curation, Conceptualization. **J.C. Gonzalez-Torres:** Writing – review & editing, Validation, Supervision, Methodology, Investigation, Funding acquisition, Formal analysis, Conceptualization. **A. Garcia-Cerrada:** Writing – review & editing, Supervision, Methodology, Conceptualization. **L. Rouco:** Writing – review & editing, Supervision, Methodology, Investigation, Formal analysis, Conceptualization. **A. Benchaib:** Writing – review & editing, Validation, Supervision, Methodology, Funding acquisition, Conceptualization. **P. Garcia-Gonzalez:** Validation, Supervision, Methodology, Conceptualization.

Declaration of competing interest

The authors declare the following financial interests/personal relationships which may be considered as potential competing interests: 1. The work described has not been published previously except in the form of a preprint, an abstract, a published lecture, academic thesis or registered report. 2. The article is not under consideration for publication elsewhere. 3. The article's publication is approved by all authors and tacitly or explicitly by the responsible authorities where the work was carried out. 4. If accepted, the article will not be published elsewhere in the same form, in English or in any other language, including electronically without the written consent of the copyright holder.

Acknowledgements

The work of Mr. Mathieu Robin is within a collaboration of SuperGrid institute in the doctoral programme of Comillas Pontifical University. It has been supported by the French Government under the program Investissements d'Avenir (ANEITE-002-01).

Appendix A. Case additional information

A.1. AC base case

Dynamic and static data of the Nordic 44 test system can be found in file `N44_BC.dyr` (folder `nordic44/models`) of `ALSETLab/Nordic44-Nordpool` [56]. The initial power flow condition used in this paper corresponds to the Nord Pool data of Tuesday November 10 at 11:38, also available in [56].

A.2. DC-segmented cases

The DC-segmented cases were obtained from the initial Nordic 44 system by replacing AC line 5100-6500 (link B) and the two parallel lines between buses 3359 and 5101 (link A) with VSC-HVDC links. The characteristics of the four VSCs and the two DC lines are included in Table A.6.

Table A.6
Data of the HVDC links in the DC-segmented Nordic 44 system.

Parameters (p.u's: converter rating)	Values
Rating VSC (VSCA1-2/ VSCB1-2)	3500/800 MVA
DC voltage (VSCA1-2/ VSCB1-2)	± 535/320 kV
Configuration	Symmetrical monopole
Max active power (VSCA1-2/ VSCB1-2)	±3500/800 MW
Max reactive power (VSCA1-2/ VSCB1-2)	±1400/320 MVAr
Max. current	1 p.u.
Max. DC voltage $V_{dc,i}^{max}, V_{dc,i}^{min}$	1.1, 0.9 p.u.
Current-controller time constant (τ)	2 ms
Connection imp. ($R_{s,i} + jX_{s,i}$)	0.004 + j 0.2 p.u.
Outer control gains	
P control	$i_{ac,d,i}^{ref} = P_{ac,i}^{*}/V_{ac,i}$
V_{dc} prop./int.($K_{p,d2}/K_{i,d2}$)	10 p.u./20 p.u./s
Q control	$i_{ac,q,i}^{ref} = -Q_{ac,i}^{*}/V_{ac,i}$
VSCs' loss coefficients	a = b = c = 0 p.u.
DC-bus capacitance ($C_{dc,i}$) (VSCA1-2/ VSCB1-2)	305/195 μF
DC-line series resistance, inductance ($R_{dc,ij}, L_{dc,ij}$)	
- link A (5101-3359)	1.6 Ω, 67 mH
- line B (5100-6500)	7.2 Ω, 258 mH

VSCs A2 (3359) and B2 (6500) were set in V_{dc}-control mode while VSCs A1 (5101) and B1 (5100) were set in P-control mode.

Parameters of Frequency Controller (FC) (Fig. 3 of Section 3.1) are $K_{FC,i} = 100$ pu, $T_{FC,i} = 0.1$ s and $\pm\Delta P_{ac,i}^{max} = \pm 1$ pu.

Data availability

Data will be made available on request.

References

[1] Luscan B, Bacha S, Benchaib A, Bertinato A, Chedot L, Gonzalez-Torres JC, et al. A vision of HVDC key role toward fault-tolerant and stable AC/DC Grids. IEEE J Emerg Sel Top Power Electron 2021;9(6):7471–85. http://dx.doi.org/10.1109/JESTPE.2020.3037016.

[2] ENTSO-E. Grid map. 2023, https://www.entsoe.eu/data/map/. Last Accessed 10 February 2023.

[3] Alassi A, Bañales S, Ellabban O, Adam G, MacIver C. HVDC transmission: technology review, market trends and future outlook. Renew Sustain Energy Rev 2019;112:530–54. http://dx.doi.org/10.1016/j.rser.2019.04.062.

[4] Gomis-Bellmunt O, Sanchez-Sanchez E, Arevalo-Soler J, Prieto-Araujo E. Principles of operation of grids of DC and AC subgrids interconnected by power converters. IEEE Trans Power Deliv 2021;36(2):1107–17. http://dx.doi.org/10.1109/TPWRD.2020.3002269.

[5] ENTSO-E. Analysis of CE inter-area oscillations of 1st December 2016. SG SPD REPORT, Brussels, Belgium: ENTSO-E; 2017.

[6] Hatziargyriou N, Milanovic J, Rahmann C, Ajjarapu V, Canizares C, Erlich I, et al. Definition and classification of power system stability – revisited & extended. IEEE Trans Power Syst 2021;36(4):3271–81. http://dx.doi.org/10.1109/TPWRS.2020.3041774.

[7] Klein M, Rogers GJ, Kundur P. A fundamental study of inter-area oscillations in power systems. IEEE Trans Power Syst 1991;6(3):914–21. http://dx.doi.org/10.1109/59.119229.

[8] Domínguez-García JL, Gomis-Bellmunt O, Bianchi FD, Sumper A. Power oscillation damping supported by wind power: A review. Renew Sustain Energy Rev 2012;16(1):4994–5006.

[9] Shah R, Mithulananthan N, Lee KY. Large-scale PV plant with a robust controller considering power oscillation damping. IEEE Trans Energy Convers 2013;28(1):106–16.

[10] Jankovic J, Roldan-Perez J, Prodanovic M, Suul JA, D'Arco S, Rouco-Rodriguez L. Power oscillation damping method suitable for network reconfigurations based on converter interfaced generation and combined use of active and reactive powers. Int J Electr Power Energy Syst 2023;149(109010):1–10.

[11] Rouco L. Coordinated design of multiple controllers for damping power system oscillations. Int J Electr Power Energy Syst 2001;23(7):517–30. http://dx.doi.org/10.1016/S0142-0615(00)00091-0.

[12] Mithulanathan N, Canizares CA, Reeve J, Rogers GJ. Comparison of PSS, SVC and STATCOM controllers for damping power system oscillations. IEEE Trans Power Syst 2003;18(2):786–92.

[13] Pierre BJ, Wilches-Bernal F, Schoenwald DA, Elliott RT, Trudnowski DJ, Byrne RH, et al. Design of the Pacific Intertie Wide Area damping controller. IEEE Trans Power Syst 2017;34(5):3594–604.

[14] Eriksson R. A new control structure for multiterminal DC grids to damp interarea oscillations. IEEE Trans Power Deliv 2016;31(3):990–8. http://dx.doi.org/10.1109/TPWRD.2014.2364738.

[15] Elizondo MA, Fan R, Kirkham H, Ghosal M, Wilches-Bernal F, Schoenwald D, et al. Interarea oscillation damping control using high-voltage DC transmission: A survey. IEEE Trans Power Syst 2018;33(6):6915–23. http://dx.doi.org/10.1109/TPWRS.2018.2832227.

[16] Renedo J, García-Cerrada A, Rouco L, Sigrist L. Coordinated design of supplementary controllers in VSC-HVDC multi-terminal systems to damp electromechanical oscillations. IEEE Trans Power Syst 2021;36(1):712–21. http://dx.doi.org/10.1109/TPWRS.2020.3003281.

[17] Gonzalez-Torres J, Mermet-Guyennet J, Silvant S, Benchaib A. Power system stability enhancement via VSC-HVDC control using remote signals: Application on the nordic 44-bus test system. In: 15th IET international conference on AC and DC power transmission. 2019, p. 1–6. http://dx.doi.org/10.1049/cp.2019.0078.

[18] Xing Y, Kamal E, Marinescu B, Xavier F. Advanced control to damp power oscillations with VSC-HVDC links inserted in meshed AC grids. Int Trans Electr Energy Syst 2021;31(12):1–26.

[19] Dong Y, Zhao Y, Alshuaibi K, Zhang C, Liu Y, Zhu L, et al. Adaptive power oscillation damping control via VSC- HVDC for the great britain power grid. In: 2023 IEEE power & energy society innovative smart grid technologies conference. Washington, DC, USA: IEEE; 2023, p. 1–5. http://dx.doi.org/10.1109/ISGT51731.2023.10066435.

[20] Li J, Liu C-C, Schneider KP. Controlled partitioning of a power network considering real and reactive power balance. IEEE Trans Smart Grid 2010;1(3):261–9. http://dx.doi.org/10.1109/TSG.2010.2082577.

[21] Hassani Ahangar AR, Gharehpetian GB, Baghaee HR. A review on intentional controlled islanding in smart power systems and generalized framework for ICI in microgrids. Int J Electr Power Energy Syst 2020;118:105709. http://dx.doi.org/10.1016/j.ijepes.2019.105709.

[22] You H, Vittal V, Wang X. Slow coherency-based islanding. IEEE Trans Power Syst 2004;19(1):483–91. http://dx.doi.org/10.1109/TPWRS.2003.818729.

[23] Sun Kai, Zheng Da-Zhong, Lu Qiang. Splitting strategies for islanding operation of large-scale power systems using OBDD-based methods. IEEE Trans Power Syst 2003;18(2):912–23. http://dx.doi.org/10.1109/TPWRS.2003.810995.

[24] Robin M, Renedo J, Gonzalez-Torres JC, García-Cerrada A, Benchaib A, García-González P. An algorithm for DC segmentation of AC power systems to mitigate electromechanical oscillations. IEEE Access 2023;11:64651–67. http://dx.doi.org/10.1109/ACCESS.2023.3287782.

[25] Clark HK, El-Gasseir MM, Kenneth Epp HD, Edris A-A. The application of segmentation and grid shock absorber concept for reliable power grids. In: 2008 12th International middle-east power system conference. Aswan, Egypt: IEEE; 2008, p. 34–8. http://dx.doi.org/10.1109/MEPCON.2008.4562303.

[26] ENTSO-E. HVDC links in system operations. Technical paper, Brussels, Belgium: ENTSO-E; 2019.

[27] Clark H, Edris A-A, El-Gasseir M, Epp K, Isaacs A, Woodford D. Softening the blow of disturbance. IEEE Power Energy Mag 2008;6(1):30–41.

[28] Fairley P. Why Southern China broke up its power grid. In: IEEE SPECTRUM. 2016, p. 13–4.
[29] Fang X, Chow JH. BTB DC link modeling, control, and application in the segmentation of AC interconnections. In: 2009 IEEE power & energy society general meeting. Calgary, Canada: IEEE; 2009, p. 1–7. http://dx.doi.org/10.1109/PES.2009.5275204.
[30] Shami UT, Naeem R, Chaudhary MS. Analysis of different power grid segmentation and transmission schemes for power system security improvement, university of engineering and technology taxila. Tech J 2015;20(I):39–49.
[31] Mousavi OA, Bizumic L, Cherkaoui R. Assessment of ?hvdc grid segmentation for reducing the risk of cascading outages and blackouts. In: 2013 IREP symposium bulk power system dynamics and control - IX optimization, security and control of the emerging power grid. Rethymno, Greece: IEEE; 2013, p. 1–10. http://dx.doi.org/10.1109/IREP.2013.6629372.
[32] Gomila D, Carreras B, Reynolds-Barredo J, Colet P, Gomis-Bellmunt O. Analysis of the blackout risk reduction when segmenting large power systems using lines with controllable power flow. Int J Electr Power Energy Syst 2023;148:108947. http://dx.doi.org/10.1016/j.ijepes.2023.108947.
[33] Cheng B, Xu Z, Xu W. Optimal DC-segmentation for multi-infeed HVDC systems based on stability performance. IEEE Trans Power Syst 2016;31(3):2445–54. http://dx.doi.org/10.1109/TPWRS.2015.2448546.
[34] El-Gasseir M, Kenneth Epp HD. Electricity market-oriented DC-Segmentation design and optimial scheduling for electrical power transmission, https://www.ic.gc.ca/opic-cipo/cpd/eng/search/number.html (Canadian Patent Application CA 2562103, PTC filling Date: 2004-03-05).
[35] Stanojev O, Garrison J, Hedtke S, Franck CM, Demiray T. Benefit analysis of a hybrid HVAC/HVDC transmission line: A swiss case study. In: 2019 IEEE milan powertech. Milan, Italy: IEEE; 2019, p. 1–6. http://dx.doi.org/10.1109/PTC.2019.8810686.
[36] Hart D, Xemard A, Poullain S, Rubinic Z, Dolenc T, Pavic K, et al. Transformation of an AC transmission line into a DC transmission line: A study case. In: CIGRE International symposium 2021 Reshaping the electric power system infrastructure. Ljubljana: CIGRE; 2021, p. 1–17.
[37] Roshanagh RG, Ravadanegh SN. A way to evaluate segmentation: An examination of AC line elimination in a parallel AC/DC transmission system. In: 2013 21st Iranian conference on electrical engineering. Mashhad, Iran: IEEE; 2013, p. 1–4. http://dx.doi.org/10.1109/IranianCEE.2013.6599651.
[38] Robin M, Renedo J, Gonzalez-Torres J-C, García-Cerrada A, Benchaib A, García-González P. DC segmentation: A promising solution to improve angle stability of stressed power systems. In: The 17th international conference on AC and DC power transmission (ACDC 2021), online conference. 2021, p. 84–90. http://dx.doi.org/10.1049/icp.2021.2449.
[39] Pirooz Azad S, Iravani R, E TJ. Dynamic stability enhancement of a DC-segmented AC power system via HVDC operating-point adjustement. IEEE Trans Power Deliv 2015;30(2):657–65.
[40] Pirooz Azad S, Iravani R, E. TJ. Stability enhancement of a DC-segmented AC power system. IEEE Trans Power Deliv 2015;30(2):737–45.
[41] Castro LM, Acha E. On the provision of frequency regulation in low inertia AC grids using HVDC systems. IEEE Trans Smart Grid 2016;7(6):2680–90. http://dx.doi.org/10.1109/TSG.2015.2495243.
[42] Zhang Q, McCalley JD, Ajjarapu V, Renedo J, Elizondo MA, Tbaileh A, et al. Primary frequency support through North American continental HVDC interconnections with VSC-MTDC systems. IEEE Trans Power Syst 2021;36(1):806–17. http://dx.doi.org/10.1109/TPWRS.2020.3013638.
[43] Shinoda K, Dai J, Bakhos G, Gonzalez-Torres JC, Benchaib A, Bacha S. Design consideration for frequency containment reserve provisions by a multi-terminal hvdc system. IET Gener, Transm Distrib 2023;17:4024–37. http://dx.doi.org/10.1049/gtd2.12955.
[44] Chompoobutrgool Y, Vanfretti L. Identification of power system dominant inter-area oscillation paths. IEEE Trans Power Syst 2013;28(3):2798–807. http://dx.doi.org/10.1109/TPWRS.2012.2227840.
[45] Cole S, Beerten J, Belmans R. Generalized dynamic VSC MTDC model for power system stability studies. IEEE Trans Power Syst 2010;25(3):1655–62. http://dx.doi.org/10.1109/TPWRS.2010.2040846.
[46] Daelemans G, Srivastava K, Reza M, Cole S, Belmans R. Minimization of steady-state losses in meshed networks using vsc hvdc. In: Proc. IEEE/PES general meeting, Calgary, AB, Canada. 2009, p. 1–5.
[47] Rouco L, Pagola FL, García-Cerrada A, Rodríguez JM, Sanz RM. Damping of electromechanical oscillations in power systems with superconduction magnetic energy storage systems: location and controller design. In: 12th Power systems computation conference, Dresden. 1996, p. 1097–104.
[48] Díez-Maroto L, Renedo J, Rouco L, Fernández-Bernal F. Lyapunov stability Based Wide Area control systems for excitation boosters in synchronous generators. IEEE Trans Power Syst 2019;34(1):194–204.
[49] Pagola F, Perez-Arriaga IJ, Verghese G. On sensitivities, residues and participations: Applications to oscillatory stability analysis and control. IEEE Trans Power Syst 1989;4(1):278–85. http://dx.doi.org/10.1109/59.32489.
[50] Larsen EV, Swann DA. Applying power system stabilizers Part II: Performance objectives and tuning concepts. IEEE Trans Power Apparatus Syst PAS 1981;100(6):3025–33.
[51] Jakobsen SH, Kalemba L, Solvang EH. The nordic 44 test network. 2018, http://dx.doi.org/10.6084/M9.FIGSHARE.7464386.V1, Online: https://figsharecom/projects/Nordic_44/57905, 1001438 Bytes.
[52] Vanfretti L, Rabuzin T, Baudette M, Murad M. iTesla power systems library (iPSL): A modelica library for phasor time-domain simulations. SoftwareX 2016;5:84–8. http://dx.doi.org/10.1016/j.softx.2016.05.001.
[53] Baudette M, Castro M, Rabuzin T, Lavenius J, Bogodorova T, Vanfretti L. OpenIPSL: open-instance power system library — update 1.5 to iTesla power systems library (iPSL): A modelica library for phasor time-domain simulations. SoftwareX 2018;7:34–6. http://dx.doi.org/10.1016/j.softx.2018.01.002.
[54] Hadjikypris M, Terzija V. Active power modulation assisting controller scheme implemented on a VSC-HVDC link establishing effective damping of low frequency power oscillations. In: Proc. IEEE international energy conference. 2014, p. 1–6.
[55] Renedo J, Díaz-García A, Torresan G, Lorenzo-Cabrera E, Cordón A, Sanz-Verdugo S, et al. Tests on the POD-P controller of INELFE Spain-France VSC-HVDC interconnector. In: Proc. CIGRE B4 international SC meeting and colloquium, Vienna, Austria, 11-15 Sep. 2023, p. 1–15.
[56] https://github.com/ALSETLab/Nordic44-Nordpool/tree/master/nordic44/models. Last Accessed 12 December 2024.